

See discussions, stats, and author profiles for this publication at: <https://www.researchgate.net/publication/235678168>

# Phase Behavior of Concentrated Suspensions of Nearly Hard Colloidal Spheres

Article in *Nature* · March 1986

DOI: 10.1038/320340a0

---

CITATIONS

2,287

---

READS

1,466

2 authors, including:



Peter Pusey

The University of Edinburgh

213 PUBLICATIONS 20,552 CITATIONS

SEE PROFILE

such a structure. This suggests that the lamellar phase is closely related to a dispersion of droplets. A transition from a dispersion of droplets to a dispersion of plates could result in a lamellar nematic-type phase. The driving force for the transition is clearly related to the alcohol content of the dispersion. Following the interfacial theory (R) presented by Winsor<sup>10</sup>, it can be argued that progressive intercalation of alcohol amongst the paraffinic surfactant chains will tend to reduce the interfacial curvature in the swollen micelle until flat regions are formed which subsequently order in a lamellar manner. This is supported by the observation that in the hexagonal and cubic phases, which have locally non-zero interfacial curvatures, the alcohol-to-surfactant ratio is less than in the lamellar phase.

Although all of the examples presented contain the same surfactant, I have also formulated liquid crystal microemulsions with other surfactants and co-surfactants. Their occurrence hence seems to be a general feature of microemulsion phase behaviour and not an isolated example.

I thank the Institut Laue-Langevin, Grenoble, for providing the neutron beam time, and S. Wilson and L. Braganza for their assistance with the D16 diffractometer.

Received 9 September 1985; accepted 21 January 1986.

1. Elkwall, P. in *Advances in Liquid Crystals* Vol. 1 (ed. Brown, G. H.) Ch. 1 (Academic, New York, 1971).
2. Tiddy, G. J. T. *Phys. Rep.* **57**, 1-46 (1980).
3. Wennerstrom, H. & Lindman, B. *Phys. Rep.* **52**, 1-86 (1979).
4. Lindman, B. & Wennerstrom, H. *Topics Curr. Chem.* **87**, 1-84 (1980).
5. Prince, L. M. *Microemulsion, Theory and Practice* (Academic, New York, 1977).
6. Cebula, D. J., Harding, L., Ottewill, R. H. & Pusey, P. N. *Colloid Polym. Sci.* **258**, 973-976 (1980).
7. Tabony, J. *Nature* **319**, 400 (1986).
8. *Neutron Beam Facilities Available for Users* (Institut Laue-Langevin, Grenoble, 1981).
9. Fontell, K. in *Liquid Crystals and Plastic Crystals* Vol. 2 (eds Gray, G. W. & Winsor, P. A.) Ch. 4 (Wiley, New York, 1974).
10. Winsor, P. A. in *Liquid Crystals and Plastic Crystals* Vol. 1 (eds Gray, G. W. & Winsor, P. A.) Ch. 5 (Wiley, New York, 1974).

## Phase behaviour of concentrated suspensions of nearly hard colloidal spheres

P. N. Pusey & W. van Megen\*

Royal Signals and Radar Establishment, St Andrews Road, Malvern WR14 3PS, UK

Suspensions of spherical colloidal particles in a liquid show a fascinating variety of phase behaviour which can mimic that of simple atomic liquids and solids. 'Colloidal fluids'<sup>1-4</sup>, in which there are significant short-range correlations between the positions of neighbouring particles, and 'colloidal crystals'<sup>5-7</sup>, which have long-range spatial order, have been investigated extensively. We report here a detailed study of the phase diagram of suspensions of colloidal spheres which interact through a steep repulsive potential. With increasing particle concentration we observed a progression from colloidal fluid, to fluid and crystal phases in coexistence, to fully crystallized samples. At the highest concentrations we obtained very viscous samples in which full crystallization had not occurred after several months and in which the particles appeared to be arranged as an amorphous 'colloidal glass'. The empirical phase diagram can be reproduced reasonably well by an effective hard-sphere model. The observation of the colloidal glass phase is interesting both in itself and because of possible relevance to the manufacture of high-strength ceramics<sup>8</sup>.

The particles studied were colloidal polymethylmethacrylate (PMMA), stabilized sterically by poly-12-hydroxystearic acid<sup>9</sup>. Electron microscopy, light scattering and crystallography showed the radius of the PMMA cores to be  $305 \pm 10$  nm and

the polydispersity (standard deviation of the particle size distribution divided by the mean size) to be about 0.05. The thickness of the stabilizer layer was 10-20 nm, a small fraction of the particle radius. Thus the repulsive potential arising from interpenetration of the polymer coatings of different particles was relatively steep. The suspension medium was a mixture of decalin and carbon disulphide in volume ratio 2.66:1, chosen to match closely the refractive index of the particles,  $\sim 1.51$  (ref. 10). This provided nearly transparent samples suitable for light scattering measurements as well as for visual observation of processes occurring in the bulk of the samples. Furthermore, index matching is expected to minimize interparticle attractions due to van der Waals forces. Ten samples were prepared from a stock solution of known PMMA weight fraction (determined by drying). They were concentrated by low-speed centrifugation to form a dense sediment, followed by removal of a weighed amount of clear supernatant liquid. Slow tumbling of the samples then redispersed the particles effectively. The fractional volumes  $\phi_c$  of the samples occupied by PMMA cores were calculated using literature values for the densities of PMMA and the liquids.

After extensive tumbling which, we assume, left the particles positionally randomized (that is, showing only local short-range order), samples 2-10 were set up as shown in Fig. 1a and were illuminated obliquely from behind by a broad beam of white light. The most dilute sample (2, on the extreme right of Fig. 1a), with  $\phi_c = 0.393$ , showed no macroscopically observable change with time. Earlier work<sup>10-12</sup> has established that at (and below) this concentration the particles are spatially arranged much like atoms in a dense liquid, exhibiting considerable short-range positional ordering. Although hindered by their neighbours, the particles remain able to diffuse through this colloidal fluid under the influence of brownian motion. After times ranging from minutes to hours, small, Bragg-reflecting crystallites formed homogeneously throughout the volumes of samples 3-7. In samples 3-5 the crystallites settled under gravity within a day to form well-defined boundaries between coexisting polycrystalline and fluid phases. Samples 6 and 7 remained filled with small compact crystallites. In these two samples the state of lowest free energy is evidently a colloidal crystal which grows, by diffusion of the particles, from the randomized metastable state formed by the tumbling process. Once crystallization is complete, the particle motions are largely limited to local brownian excursions centred on sites in the regular crystalline array. The crystal structure was determined by light-scattering crystallography to be face-centred cubic<sup>13</sup>. The coexistence of colloidal fluid and crystal observed in samples 3-5 is analogous to the coexistence of a simple liquid and solid (such as ice and water) at a first-order phase transition. Sample 8 crystallized heterogeneously, starting from the meniscus and cell walls, to form relatively large irregular crystals. The most concentrated ( $\phi_c \geq 0.50$ ), highly viscous samples 9 and 10 exhibited only partial heterogeneous crystallization even when left undisturbed for several months. Although the crystalline state is, presumably, still thermodynamically preferred for these samples, it appears that the concentration is so high that particle diffusion is hindered to the point where crystals do not form on this timescale and the suspensions remain in the metastable amorphous phase created by the tumbling. The different results of homogeneous and heterogeneous nucleation are shown clearly in Fig. 1b.

The observed phase behaviour is summarized in Fig. 2. In the coexistence region we plot the fraction of the sample volume occupied by the crystalline phase against  $\phi_c$ . Not surprisingly, we find a linear (lever-rule) dependence which, when extrapolated to 0 and 100%, provides 'freezing' and 'melting' concentrations.

While there is evidence<sup>13</sup> that, due to interpenetration of their stabilizing polymer coatings, the interaction between the particles is slightly 'soft', it seems simplest to discuss our findings in terms of an effective hard-sphere model; such models for simple

\* Permanent address: Department of Applied Physics, Royal Melbourne Institute of Technology, Melbourne, Australia.

**Fig. 1** *a*, Nearly-hard-sphere suspensions, 4 days after tumbling, illuminated obliquely from behind by white light. The samples are contained in cells of cross-section  $1\text{ cm} \times 1\text{ cm}$  and are numbered 2–10, in our nomenclature, from the right in order of increasing concentration. Actual concentrations are shown in Fig. 2. Immediately after tumbling, all the samples appeared featureless (see top of sample 2 or bottom of sample 9), reflecting randomization of the particle positions. The text describes the dynamic processes which occurred over 4 days and led to the structures depicted in the photograph. The scattering geometry is such that the first peak in the structure factor of the amorphous phases and the first Bragg reflection of the crystals occur in the red at the right of the picture and in the blue-green at the left. Some overall gravitational settling of the particles has occurred, leading to a small layer of crystals at the bottom of sample 2 (which, it should be emphasized, showed no crystallization in the bulk) and compaction of the crystallites at the bottom of samples 3–7. *b*, Close-up of samples 7–9 under the same conditions as in *a*. Crystallization nucleated homogeneously in sample 7 but heterogeneously in sample 8. The lower part of sample 9 shows clearly the amorphous glassy phase which did not crystallize over several months.



liquids have been extensively studied, both theoretically and by computer simulation<sup>14–17</sup>. Thus we assume that the core volume fraction  $\phi_C^E = 0.407$ , at which freezing starts (see Fig. 2), is equivalent to an effective volume fraction 0.494, the freezing concentration for hard spheres<sup>16</sup>. This implies a hard-sphere interaction radius about 20 nm (roughly the thickness of the stabilizer layer) greater than the core radius,  $\sim 305\text{ nm}$ . We therefore include in Fig. 2 a scale appropriate to the effective hard-sphere volume fraction, defined by  $\phi_E = (0.494/0.407) \phi_C$ . With this scaling the melting density  $\phi_E^M = 0.536$  for the colloidal suspension is slightly smaller than the value 0.545 expected for the equivalent hard spheres<sup>16</sup>. Such a slight difference between the observed coexistence region and that expected for hard spheres could be caused by several factors; for example, softness

of the interparticle potential<sup>17</sup>, slight interparticle attractions<sup>17</sup>, particle polydispersity<sup>18</sup>, or, very likely, a combination of these. The effective volume fraction of the most concentrated glassy sample, 10, is close to the value  $\phi_E = 0.637$  expected for the Bernal (random close-packed) hard-sphere glass<sup>14,19,20</sup>.

We conclude that the colloidal suspensions described above should prove useful model 'nearly-hard-sphere' systems for further experimentation. In particular, the rate of transport in these suspensions is many orders of magnitude smaller than that in simple molecular systems, a property which should simplify the study of some kinetic processes<sup>21</sup>. We have already made a number of other measurements, discussed elsewhere<sup>13</sup>. These include: the kinetics of crystallization, light crystallography, rheological measurements in the metastable fluid and



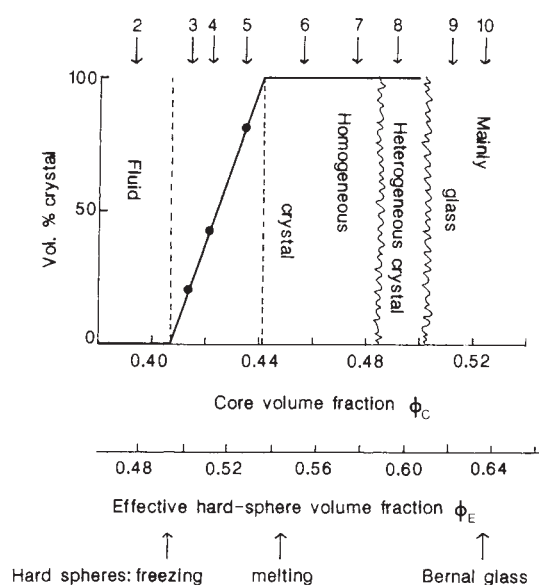


**Fig. 2** 'Phase-diagram' of the samples shown in Fig. 1. Arrows at top indicate the sample concentrations. The two horizontal axes indicate the measured volume fraction of PMMA cores and the effective hard-sphere volume fraction defined in the text. Arrows at the bottom indicate the volume fractions, obtained from computer simulations, for freezing, melting and random close packing ('Bernal glass') of hard spheres.

glassy phases, and measurements by conventional and dynamic light scattering of structure factors and particle diffusion in the fluid, crystal and glassy phases. The discovery of a glass composed of (nearly) equal-sized spheres is especially interesting since, although there has recently been considerable theoretical work (for example, refs 22–25) and computer simulations<sup>14,15</sup> on such model glasses, real glasses composed of spherical units are rare. (Colloidal glasses observed up to now have contained mixtures of spheres of different sizes<sup>26</sup>.) Finally we note current interest<sup>8</sup> in manufacturing industrial ceramics from 'green bodies' composed of particles of uniform size packed densely either at random (a colloidal glass) or in a colloidal crystal; the present work shows how both these structures may be achieved.

We thank Professor R. H. Ottewill and his group at Bristol University for providing the PMMA particles complete with electron-microscopic characterization; Dr L. V. Woodcock for a valuable discussion; and Mr L. Clarke for the photography.

Received 13 November 1985; accepted 5 February 1986.

1. Brown, J. C., Pusey, P. N., Goodwin, J. W. & Ottewill, R. H. *J. Phys. A* **8**, 664–682 (1975).
2. Dickinson, E. A. *Rep. R. Soc. Chem. C*, 3–37 (1983).
3. van Megen, W. & Snook, I. *Adv. Colloid Interface Sci.* **21**, 119–194 (1984).
4. Edwards, J., Everett, D. H., O'Sullivan, T., Pangalou, I. & Vincent, B. *JCS Faraday Trans. I*, **80**, 2599–2607 (1984).
5. Kose, A. & Hachisu, S. *J. Colloid Interface Sci.* **46**, 460–469 (1974).
6. Clark, N. A., Hurd, A. J. & Ackerson, B. J. *Nature* **281**, 57–60 (1979).
7. Pieranski, P. *Contemp. Phys.* **24**, 25–73 (1983).
8. Calvert, P. *Nature* **317**, 201 (1985).
9. Antl, L. *et al. Colloids and Surfaces* (in the press).
10. van Megen, W., Ottewill, R. H., Owens, S. M. & Pusey, P. N. *J. chem. Phys.* **82**, 508–515 (1985).
11. Pusey, P. N. & van Megen, W. *J. Phys., Paris* **44**, 285–291 (1983).
12. Vrij, A. *et al. Faraday Discuss. chem. Soc.* **76**, 19–35 (1983).
13. Pusey, P. N. & van Megen, W. in *Proc. Symp. Physics of Complex and Supermolecular Fluids* (ed. Safran, S. A.) (Wiley, New York, in the press).
14. Woodcock, L. V. *Ann. N.Y. Acad. Sci.* **37**, 274–298 (1981).
15. Angell, C. A., Clarke, J. H. R. & Woodcock, L. V. *Adv. chem. Phys.* **48**, 397–453 (1981).
16. Hoover, W. G. & Ree, F. H. *J. chem. Phys.* **49**, 3609–3617 (1968).
17. Hansen, J. P. & McDonald, I. R. *Theory of Simple Liquids* (Academic, New York, 1976).
18. Dickinson, E. & Parker, R. J. *J. Phys., Paris* **46**, L229–L232 (1985).
19. Bernal, J. D. & Mason, J. *Nature* **188**, 910 (1960).
20. Bernal, J. D. *Proc. R. Soc. A* **280**, 299–322 (1964).
21. Hanley, H. J. M., Rainwater, J. C., Clark, N. A. & Ackerson, B. J. *J. chem. Phys.* **79**, 4448–4458 (1983).
22. Leutheusser, E. *Phys. Rev. A* **29**, 2765–2773 (1984).
23. Das, S. P., Mazenko, G. F., Ramaswamy, S. & Toner, J. *J. Phys. Rev. Lett.* **54**, 118–121 (1985).
24. Singh, Y., Stoessel, J. P. & Wolynes, P. G. *Phys. Rev. Lett.* **54**, 1059–1062 (1985).
25. Ullio, J. J. & Yip, S. *Phys. Rev. Lett.* **54**, 1509–1512 (1985).
26. Lindsay, H. M. & Chaikin, P. M. *J. chem. Phys.* **76**, 3774–3781 (1982).

## Bubble raft model for indentation with adhesion

J. M. Georges, G. Meille, J. L. Loubet & A. M. Tolen

Laboratoire de Technologie des Surfaces, Ecole Centrale de Lyon, 36 avenue Guy de Collongue, CNRS UA 85, BP 163, 69131 Ecully Cedex, France

Indentation hardness tests are now widely used to measure the mechanical properties of solid surfaces<sup>1–3</sup>. Recent developments of this technique<sup>4,5</sup> permit the analysis of the outermost 10 nm of materials. Experimental and theoretical questions arise regarding the physical and mechanical processes involved in such small indentations. We describe here an indentation experiment on a microscopic scale, using soap bubbles blown onto a water surface. Bubble rafts provide a simple two-dimensional model for indentation behaviour; as for other materials, their behaviour is governed by two principal attraction–repulsion forces<sup>6</sup>, and by geometrical constraints. A crystalline two-dimensional lattice is obtained by using bubbles of uniform size<sup>7–9</sup>, whereas bubbles of two sizes give an amorphous structure<sup>10,11</sup>. Indentation can be represented by the contact between a triangular crystalline raft and a rectangular crystalline raft bordered by an amorphous layer. The flow of the materials, which is dependent on both adhesion and the force between the two rafts, can be analysed during the experiment.

The experimental configuration is shown in Fig. 1. We used a rectangular glass trough, approximately 60 × 30 cm and 15 cm deep, containing a soap solution of surface tension  $\gamma = 6.9 \times 10^{-2} \text{ N m}^{-1}$ . Air at constant pressure was blown through short capillaries with 50- $\mu\text{m}$  and 100- $\mu\text{m}$  bores in order to produce uniform bubbles. The bubble diameter depends on the nozzle size and is independent of the distance of the jet below

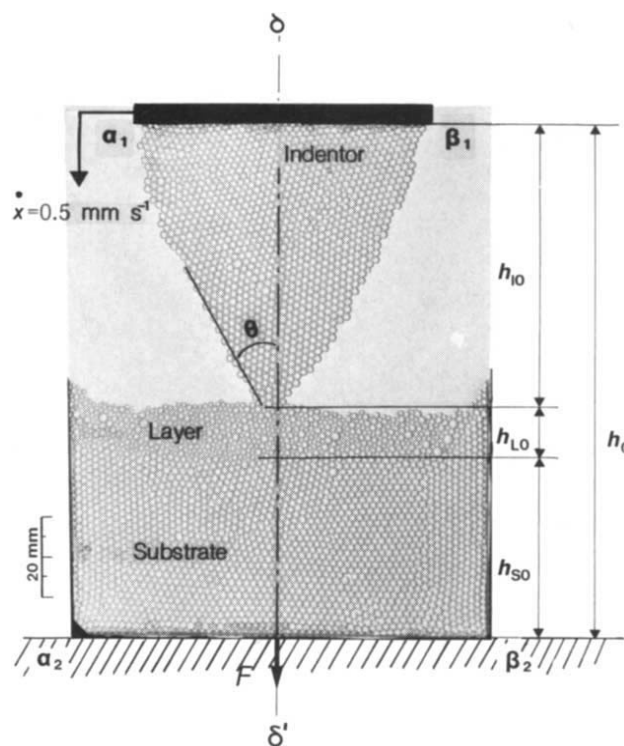


**Fig. 1** Bubble rafts used to model the indentation process. Two-dimensional rafts containing bubbles of 2.3 mm and 1.4 mm diameter are blown onto a water surface. The displacement to frame  $\alpha_1\beta_1$  parallel to frame  $\alpha_2\beta_2$  causes indentation to take place. The force  $F$  is measured in the plane perpendicular to frame  $\alpha_2\beta_2$ .